


The combined impact of fisheries and climate change on future carbon sequestration by oceanic macrofauna

Received: 7 May 2025

Accepted: 22 September 2025

Published online: 27 October 2025

 Check for updatesGaël Mariani^{1,2}✉, Jérôme Guet³, Daniele Bianchi³, Tim DeVries^{4,5}, Nicolas Barrier¹, Marc Troussellier¹ & David Mouillot¹

Although the role of marine macrofauna in the ocean carbon cycle is increasingly understood, the cumulative impacts of fisheries and climate change on this pathway remain overlooked. Here, using a marine ecosystem model, we estimate that each degree of warming reduces macrofauna biomass and carbon export by 4.2% and 2.46%, respectively. Under a high emission scenario (SSP 5–8.5), this translates to a $13.5 \pm 6.6\%$ decline in export by 2100, relative to the 1990s. Fishing further amplifies this reduction by up to $56.7 \pm 16.3\%$, creating a sequestration deficit of 14.6 ± 10.3 GtC by 2100. On average, a 1% biomass loss from fishing results in a 0.8% decline in carbon export. However, sequestration durability (~600 years) remains unaffected. While measures restoring commercial macrofaunal biomass could yield carbon benefits comparable to mangrove restoration, multiple uncertainties limit their inclusion in the Nature-based Climate Solution portfolio, highlighting the need for further research.

In the 6th Assessment Report, the Intergovernmental Panel on Climate Change (IPCC) concludes that, along with a stringent reduction in emissions, Nature-based Climate Solutions (NbCS) are needed to achieve a net-zero CO₂ emissions target¹. NbCS mainly consider protecting, managing, and restoring natural ecosystems to increase carbon sequestration or to reduce their CO₂ emissions². Terrestrial NbCS have a large climate mitigation potential^{3,4}, but the durability of their carbon sequestration is imperiled by increasing climate-related threats such as droughts and wildfires^{5–9}. By contrast, the sequestration potential of marine macrofauna and its vulnerability to ongoing global changes are unknown.

In the ocean, biological activity takes up 52.9 ± 9.1 GtC yr⁻¹ from surface waters in contact with the atmosphere¹⁰. Of these, 8.2 ± 2.8 GtC yr⁻¹ are exported from the base of the euphotic zone (~100 m)¹⁰ and sequestered in the ocean interior from decades to centuries depending on the carbon origin^{11,12}. Fish plays an important role in this ‘biological pump’, accounting for 16.1% (±13%) of the carbon exported¹³ and around 28⁶⁶% of the biogenic carbon sequestered in the ocean

interior¹². The carbon sequestration potential of fish is enhanced by the fast-sinking fecal pellets and carcasses that these organisms produce, which efficiently transfer carbon deep into the ocean, where it is ultimately consumed, respired, and stored as CO₂ for centuries¹².

Despite the importance of fish to the ocean’s biological carbon pump, our understanding of how fisheries and climate change affect the carbon cycle remains limited^{14,15}, and the extent to which protection, restoration, and management efforts can enhance carbon export and sequestration is still unclear^{16,17}. At present, it is well established that fisheries have directly reshaped the living carbon stock, altered the body size spectrum of marine macrofauna¹⁸, and substantially reduced their commercial biomass. For example, a recent study estimates a 3-fold macrofaunal biomass reduction in the ocean from the preindustrial period (3.3 ± 0.5 Gt) to present (1.1 ± 0.2 Gt)¹⁹. Ocean warming has also directly impacted marine macrofauna and has contributed to a 4.1% average biomass decrease for assessed stocks over the period 1930–2010²⁰. Meanwhile, projections based on an ensemble of marine ecosystem models (MEMs)

¹MARBEC, Univ Montpellier, CNRS, Ifremer, IRD, Montpellier, France. ²Sasakawa Global Ocean Institute, World Maritime University, Malmö, Sweden.

³Department of Atmospheric and Oceanic Sciences, University of California Los Angeles, Los Angeles, CA, USA. ⁴Department of Geography, University of California, Santa Barbara, CA, USA. ⁵Earth Research Institute, University of California, Santa Barbara, CA, USA. ✉e-mail: gael-mariani@hotmail.com

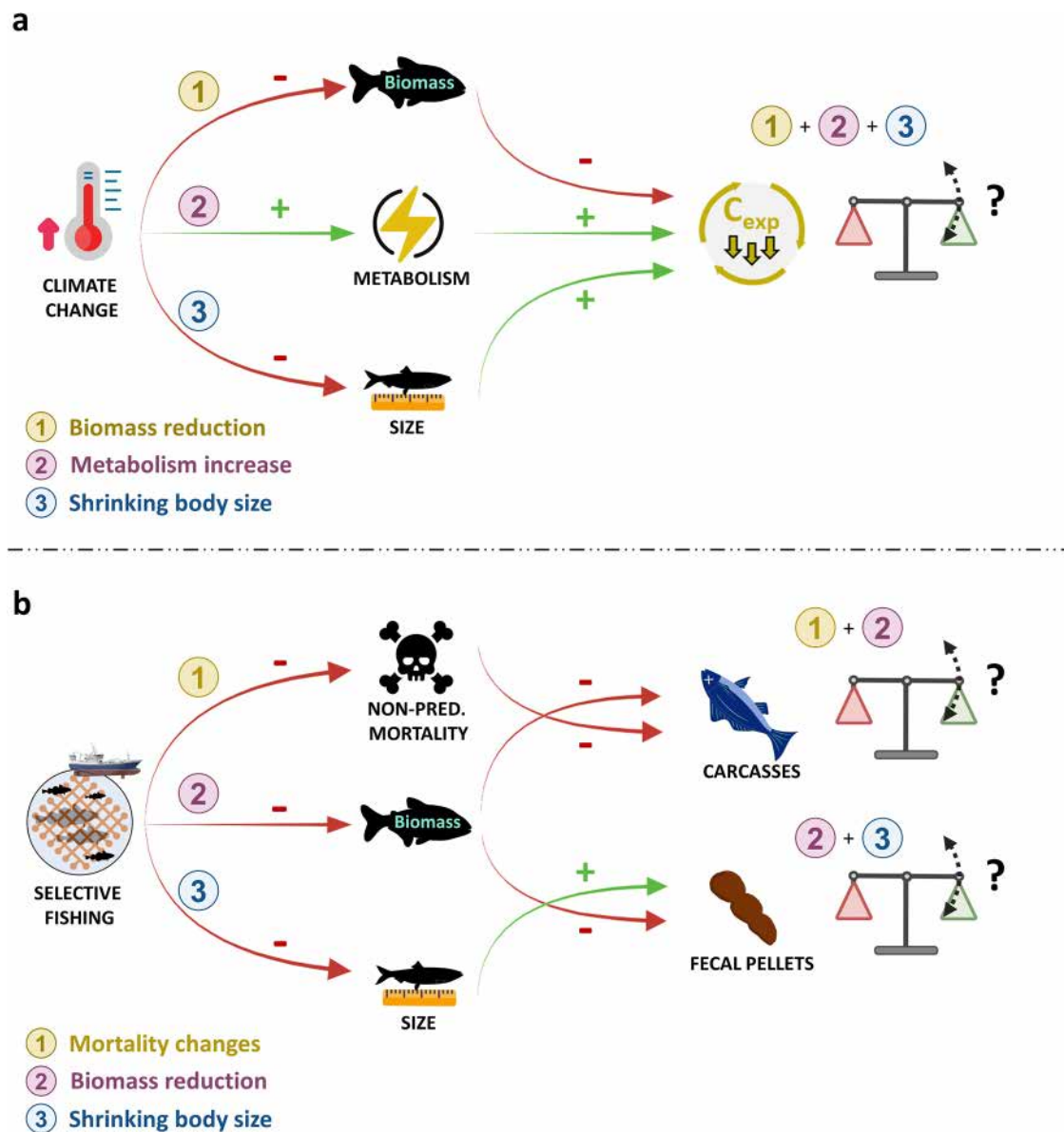


Fig. 1 | Hypothesized mechanisms of climate change and fisheries impacts on marine macrofauna biomass and carbon export. Green (red) arrows represent an increase (decrease) in the pointed process or biological component. The scales on the right represent trade-offs between positive (green weights) and negative effects (red weights) of climate change and fisheries on carbon export. **a** Schematic representation of the mechanisms leading to a smaller decline in carbon export compared to the decline in biomass. Pathway 1 only considers the impact of biomass reduction on carbon export. Pathway 2 accounts for metabolism acceleration under warmer temperatures, inducing an increase in consumption and fecal pellet production. Pathway 3 combines the reduction of organisms' body size under a warmer environment and the hypoallometric relationship between body size and consumption, i.e., at equal biomass, small individuals consume more food compared to large ones. Pathways 2 and 3 can partly counterbalance the direct effects of biomass reduction (Pathway 1). **b** Schematic representation of the mechanisms

leading to a smaller decline in fecal pellet production compared to the decline in carcass production. The combination of Pathway 1 (fishing larger individuals leads to a decrease in the size of individuals and a decrease in the non-predation mortality rate, which is size dependent, see Eqs. 18) and 2 (reduced biomass due to selective fishing) leads to a decline in carcass production close to the decline in biomass because no compensatory mechanisms are at play. In parallel, the reduction in biomass (Pathway 2) is slightly offset by the hypoallometric relationship between body size, consumption, and fecal pellet production (Pathway 3). Consequently, the decrease in fecal pellet production is lower compared to that of carcass production. Created in BioRender. Mariani, G. (2025) <https://BioRender.com/gu4y4c3>. Icons made by Good Ware, Muhammad Atif, Freepik, and heisenberg_jr from www.flaticon.com. Icon created in BioRender. Mariani, G. (2025) <https://BioRender.com/8hxgiqu>.

suggest further biomass reductions of $5\% \pm 4\%$ and $17\% \pm 11\%$ by 2100 under low (RCP 2.6) and high (RCP 8.5) emission scenarios, respectively^{21,22}. The impact of these macrofaunal biomass declines on carbon export and sequestration is not necessarily straightforward (Fig. 1). While a biomass reduction due to climate change and fisheries might lead to a decrease in carbon export from sinking fecal pellets¹⁹ and carcasses²³ (respectively Fig. 1a–Pathway 1, Fig. 1b–Pathway 2), compensatory mechanisms such as increasing carbon

ingestion and production of fecal pellets due to the temperature dependency of macrofauna metabolism²⁴ may promote carbon export and partly offset the expected decline (Fig. 1a). Moreover, changes in size structure such as the shrinking of organisms with increasing temperature²⁵, or fishing practices that target large individuals¹⁸, can also compensate the effect of declining biomass. This is because at equal biomass, small individuals consume more food compared to large ones²⁴ (respectively Fig. 1a, b–Pathway 3).

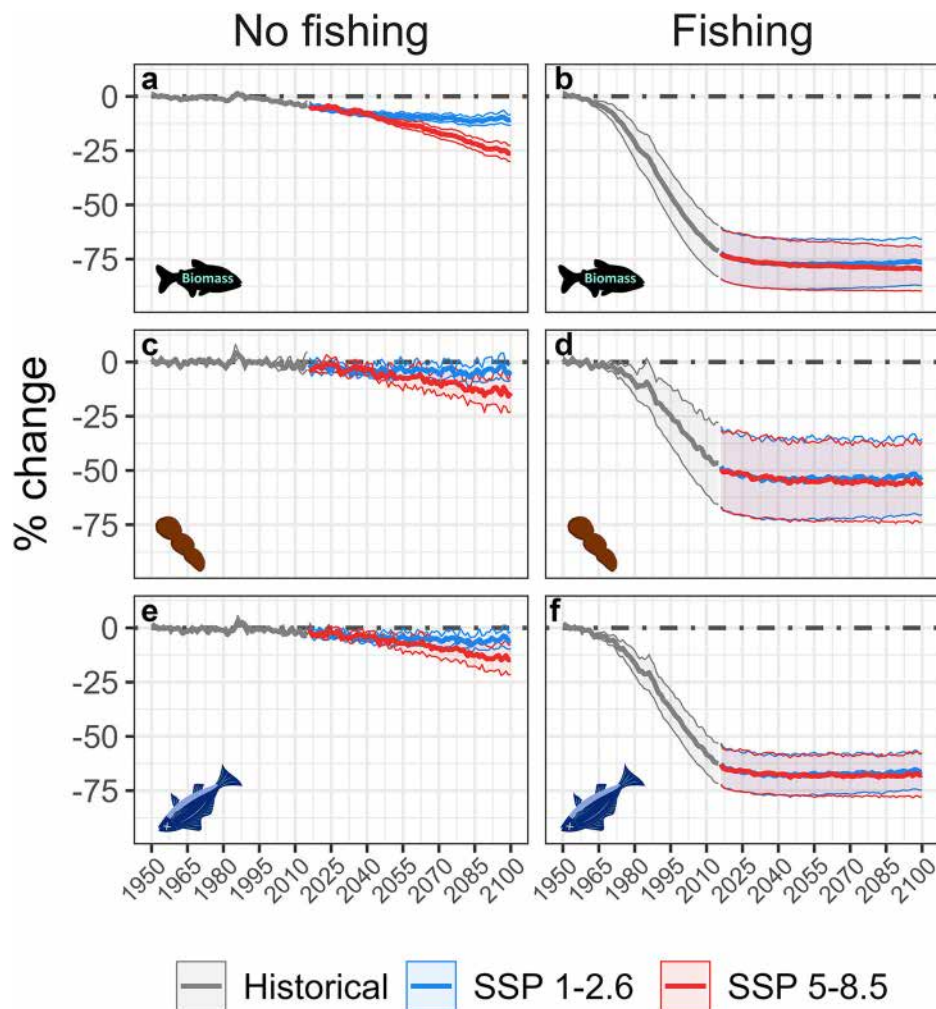


Fig. 2 | Impacts of climate change and fishing on commercial macrofauna biomass and related carbon export. BOATS ensemble projections of global change (%) in carbon stock (biomass), fecal pellets and carcasses production in the absence (a, c, e) and presence (b, d, f) of fishing, with and without climate change (SSP 1-2.6 in blue and SSP 5-8.5 in red), relative to the reference period (1950–1959). In b, d, f (red curves), fishing mostly affects the historical period because fishing is

kept constant after 2014, while climate change mostly affects the future trends. The thick solid lines represent the average value, while shading represents the standard deviation calculated from BOATS simulations for the five sets of parameters and forced with two ESM ($n = 10$, see “Methods” section). Icon created in BioRender. Mariani, G. (2025) <https://BioRender.com/8hxgiqu>.

Ultimately, better understanding and quantifying the extent to which climate change and fisheries may impact the contribution of marine macrofauna to carbon export and sequestration are essential for its potential inclusion in future oceanic NbCS.

Here, we used the BiOeconomic mArine Trophic Size-Spectrum (BOATS)^{19,26–28} model to explore the influence of fisheries and climate change on the biomass of commercial marine macrofauna (animal organisms with body size ranging from 10 g to 100 kg, primarily including fish but also encompassing invertebrates such as squids, hereafter referred to as macrofauna), their carbon export via fecal pellets and carcasses, and the resulting carbon sequestration in the ocean interior (see Supplementary Tables 1–3 for main model parameters and variables). We compared two contrasting scenarios to account for the impact of climate change: the low-emission (shared-socioeconomic pathway (SSP) 1–2.6) and the high-emission (SSP 5–8.5) scenarios. Each simulation, covering the historical period (1950–2014) and future projections (2015–2100), used two variables to force the model (see “Methods” section): net primary production (NPP) and sea surface temperature (SST), both derived from two earth system models (ESM). To explore the cumulative impact of climate change and fisheries, we ran climate change scenarios with and without fishing effort, following the Fisheries and Marine Ecosystem Intercomparison

Project (FishMIP) protocol^{22,29}. The BOATS model considers fishing effort dynamically to reproduce historical catch up to year 2014²⁸, while this effort is kept constant in future projections till 2100. To account for the uncertainty in biological processes and their interaction with fishing, which ultimately control biomass accumulation, fecal pellet production, and carcass generation, we performed five BOATS simulations for each climate and fishing scenario, using five distinct sets of parameters to reflect parameter uncertainty (as in Galbraith et al.²⁸, Supplementary Table 3). As the macrofauna considered here do not conduct significant vertical migrations, we assumed that the carbon respired by commercial species is injected into surface waters, where it can quickly exchange with the atmosphere, and is therefore unlikely to influence carbon sequestration. Moreover, mesopelagic fish, which likely contribute significantly to the oceanic carbon cycle¹², are not accounted for in this study, as they are not currently considered species of commercial interest. We assessed the present-day and future contributions of marine macrofauna to oceanic carbon sequestration, including sequestration time, using an ocean circulation inverse model (OCIM)³⁰. Acknowledging the limitations of using a single MEM, we further compared BOATS results with simulations from 5 additional MEMs included in FishMIP²² (see list in Supplementary Table 4). We also compared BOATS results to global observational

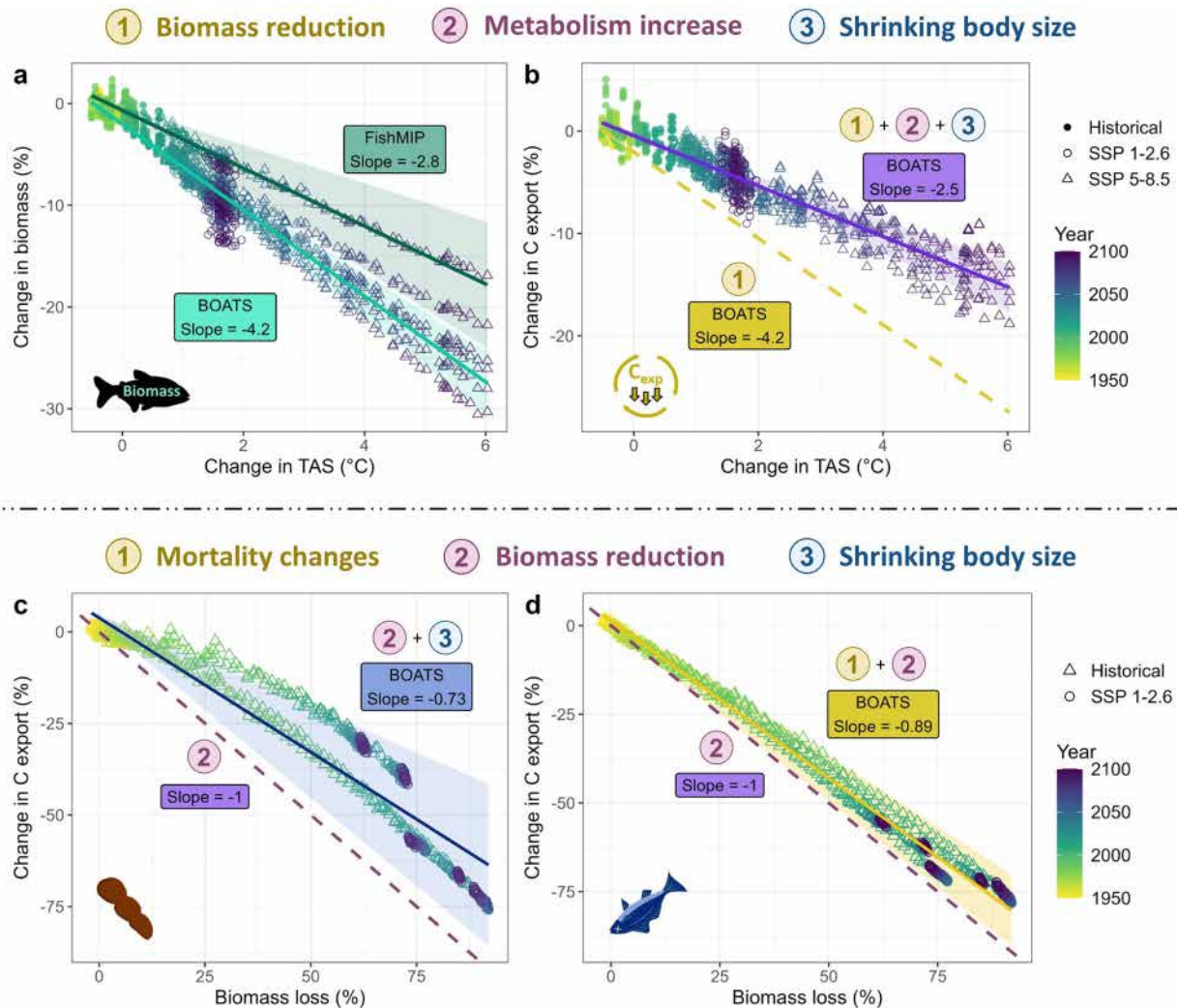


Fig. 3 | Projected impacts of climate change and fishing on macrofauna biomass and carbon fluxes. Projected changes in macrofauna biomass (a) and carbon export (b) as a function of change in global near-surface air temperature (TAS) under SSP 1–2.6 and SSP 5–8.5 scenarios. Changes are estimated annually relative to a reference period (1990–1999). In (a), FishMIP mean biomass outputs and the associated standard deviation (shaded blue areas) are plotted for comparison with BOATS outputs. Projected changes in macrofauna fecal pellets (c) and carcasses (d) export as a function of projected change in biomass, under a scenario with

fishing. Changes are estimated annually relative to a reference period (1950–1959). In b–d, the dashed lines represent the hypothesized loss in carbon export when only driven by the change in biomass. Full lines in (b–d) represent the losses in carbon export when the mechanisms described in Fig. 1 are also taken into account, highlighting the compensatory mechanisms at play. In all panels, the thick solid lines represent the average value, shaded areas represent standard deviations, and each dot represents an annual ensemble mean of BOATS outputs. Icon created in BioRender. Mariani (2025) <https://BioRender.com/8hxgiqu>.

reconstructions based on stock assessment data³¹ to illustrate the range of potential fishing impacts on macrofauna biomass.

Results and discussion

Macrofauna biomass under global change scenarios

In a scenario without fishing, climate change alone is projected to impact marine macrofauna biomass. By the end of the century, BOATS simulations project a decrease in the biomass of $9.4\% \pm 2.8\%$ and $23.9\% \pm 3.6\%$ relative to the reference period (1990–1999), under a low and high emissions scenario, respectively (Fig. 2a and Supplementary Table 5). In BOATS, historical fishing pressure substantially reduces the carbon biomass of living macrofauna from 0.56 ± 0.29 GtC in 1950, down to 0.13 ± 0.045 GtC in 2010, so a $70.9\% \pm 11.6\%$ decrease compared to the reference period (1950–1959) (Fig. 2b and Supplementary Table 5). By the end of the century, the large decline of macrofauna biomass ($-77.2 \pm 10.2\%$ relative to 1950–1959) suggests a stronger impact of global fisheries compared to climate alone.

Carbon export under global change scenarios

In the 1950s, we estimate that the marine macrofauna of commercial interest exported a total of 0.23 ± 0.11 GtC yr⁻¹ (Supplementary Table 6), slightly larger than the previous estimate from ref. 12 of 0.16 GtC yr⁻¹. More than 90% of this export (-0.21 ± 0.1 GtC yr⁻¹) originates from fecal pellets production, while the rest, 0.02 ± 0.006 GtC yr⁻¹, is due to sinking carcasses (Supplementary Table 6). Although the range of our estimates for fecal pellets export encompasses the value reported by Pinti et al.¹², our assessment for carcasses is one order of magnitude higher than Pinti et al.¹². Climate change alone is projected to decrease carbon export via fecal pellets production by $3.5\% \pm 4.3\%$ under SSP 1–2.6, and $13.5\% \pm 6.6\%$ under SSP 5–8.5 by the end of the century (Fig. 2c and Supplementary Table 6), compared to the reference period (1990–1999). The projected decrease for carcasses reaches $4.59\% \pm 4.32\%$ and $13.3\% \pm 6.38\%$ by the end of the century, under SSP 1–2.6 and SSP 5–8.5, respectively (Fig. 2e and Supplementary Table 6). Given the projected decline in biomass due to climate change, we expect a decrease in carbon export; yet, the

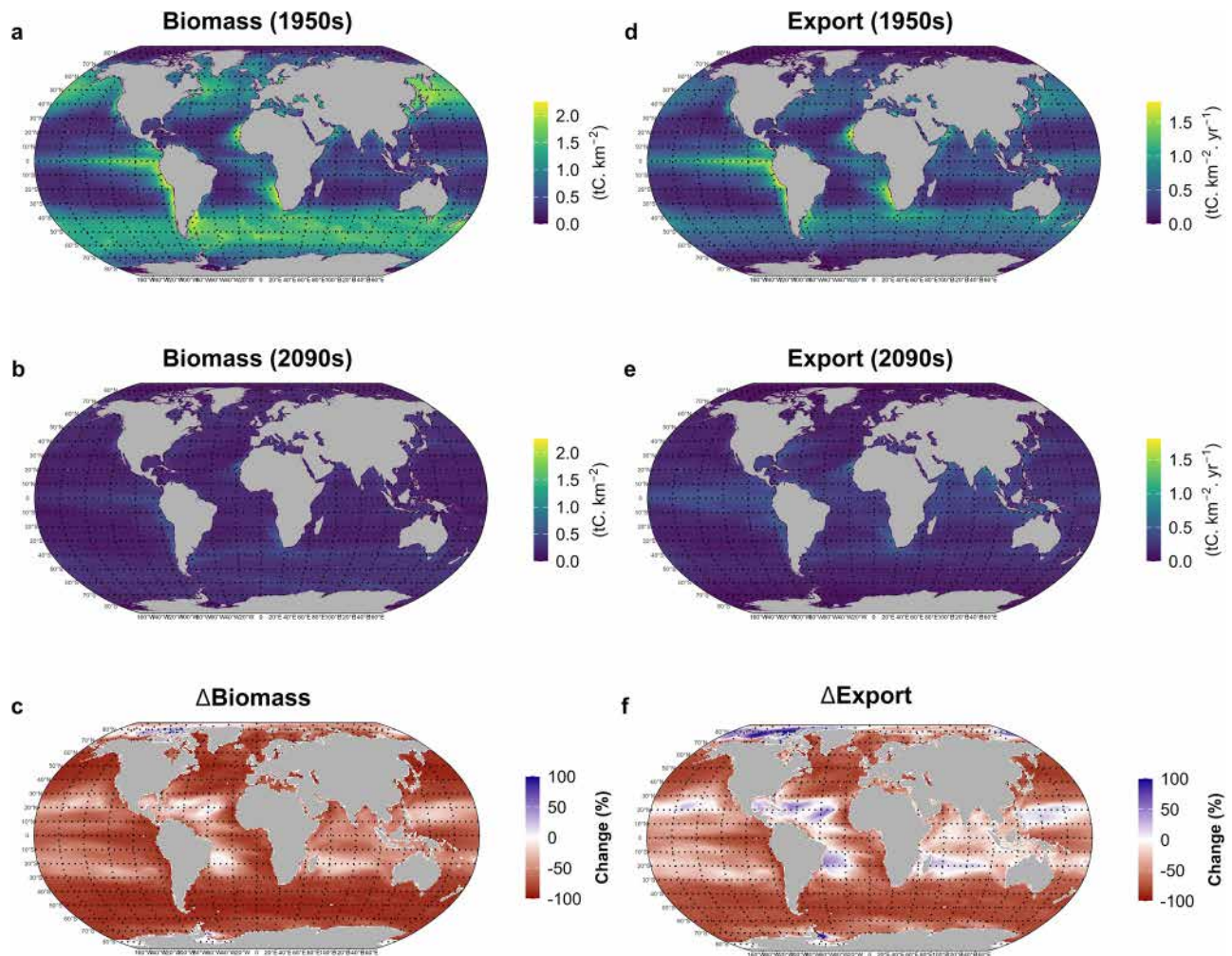


Fig. 4 | Projected spatio-temporal changes in macrofauna biomass and carbon export at the global scale. Cumulative projected impacts of climate change (SSP 5–8.5) and fisheries on macrofauna biomass (**a, b**) and carbon export (**d, e**) for the

1950s (**a, d**) and the 2090s (**b, e**) periods, and the projected changes (%) between these two periods (**c, f**). For panels **a, b, d, e**, we used a log+1 transformation of the data.

increase in temperature-dependent metabolism with warming, as well as the shrinking in body size, would mitigate this decline (Fig. 1a–Pathways 2 and 3). Indeed, higher temperatures induce faster growth and higher consumption rates, increasing fecal pellet production. This effect is amplified by the hypoallometric relationship between organisms' consumption rate and body mass³², since individual body size decreases with climate change²⁵. BOATS simulations estimate a decrease in biomass of 4.22% [95% CI: 4.14; 4.3] for every 1°C of warming, significantly higher than the decrease in carbon export of 2.46% [95% CI: 2.38; 2.54] (Fig. 3a, b, p -value < 0.0001, Supplementary Table 7). Historical fishing reduces the total carbon export in the 2010s to 0.12 ± 0.037 GtC yr⁻¹, corresponding to a decrease of -47% compared to the reference period (1950–1959). Fishing has a bigger impact on the export of carcasses compared to that of fecal pellets, with a $-62\% \pm 9\%$ and $-47.2\% \pm 17.6\%$ decrease, respectively (Fig. 2d, f and Supplementary Table 6). More than the direct effect of biomass reduction on carbon export, fishing is also expected to indirectly impact carbon export through its effects on the macrofauna size spectrum, with a shift towards smaller individuals¹⁸. In relative terms, the decline in carbon export from carcasses can have the same magnitude as the loss of macrofauna biomass because the decline in carcass production by larger individuals is expected to be almost equivalent in magnitude to the biomass decline induced by fishing (Fig. 1b–Pathway 1, and Supplementary Figs. 4–8). In contrast, smaller organisms are less affected by fisheries, and because they produce

more fecal pellets per unit of biomass compared to larger organisms²⁴, the shift in body size distribution could mitigate the loss of fecal pellets export, compared to the loss of carcasses export and biomass (Fig. 1b). Using BOATS simulations in a scenario with fishing, carbon export from dead carcasses decreases significantly more than fecal pellets exports (p -value < 0.0001, Supplementary Table 7), with a respective drop by 0.89% [95% CI: 0.9; 0.87] and 0.73% [95% CI: 0.74; 0.72] for every percent of macrofauna biomass decrease (Fig. 3c, d).

By the end of the century, the combined impacts of climate change and fishing is primarily dominated by that of fishing (Fig. 2). By the 2090s, the combined impacts would induce a decline in carbon export of $53.9\% \pm 16.5\%$ and $67\% \pm 8.63\%$ for fecal pellets and carcasses, respectively (Supplementary Table 6), relative to the period 1950–1959. Overall, the deficit in carbon export, from 1950 to 2014, reached 3.2 ± 2.6 GtC, with 89% of this deficit (2.9 ± 2.5 GtC) coming from the loss of fecal pellet production. Under contemporary fishing effort and SSP 5–8.5, an additional deficit of 11.4 ± 7.7 GtC would be added to the historical deficit, totaling a cumulative export loss of -14.6 ± 10.3 GtC by 2100. This is equivalent to 1.3 years of global emissions, based on the annual emissions estimated at 42 GtCO₂ in 2024³³.

Contextualization of BOATS results with other models

Because using a single MEM to assess the impact of climate change on macrofauna biomass and carbon export involves uncertainties

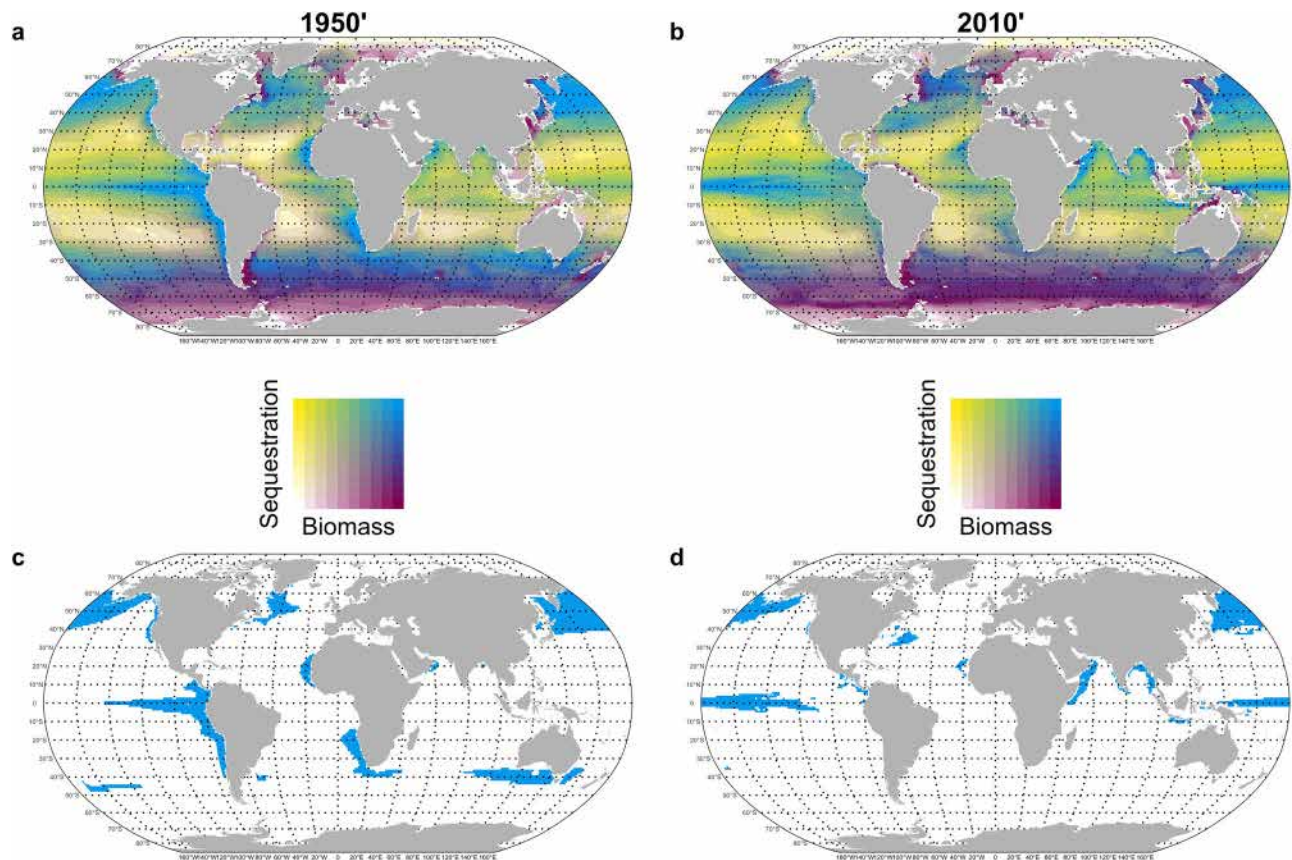


Fig. 5 | Spatial reduction in oceanic KMCA over time. a, b Bivariate map of marine macrofauna contribution to carbon sequestration as a function of macrofauna biomass for the 1950s (a) and the 2010s (b). Colors represent the quantiles of each component. **c, d** Identification of oceanic KMCA using an upper quartile

method in the 1950s (c) and the 2010s (d). KMCA corresponds to both high macrofauna biomass and high contribution of marine macrofauna to carbon sequestration.

inherent to model design, we contextualize BOATS biomass projections using simulations from five other MEMs (hereafter called the FishMIP ensemble, see list and references in Supplementary Table 4). Compared to the FishMIP ensemble mean, BOATS simulations project a slightly greater impact of climate change on macrofauna biomass, with a decrease that falls at the higher end of the FishMIP ensemble range (Supplementary Figs. 1 and 2). BOATS predicts a decrease of $9.4\% \pm 2.8\%$ and $23.9\% \pm 3.6\%$ by the end of the century, relative to the reference period (1990–1999), under a low and high emissions scenario, respectively, when the FishMIP ensemble projects a decrease by 5.79% [3.04, 8.58] and 15.8% [9.96, 21.8] (Supplementary Table 5 and Supplementary Figs. 1 and 2). Hence, for every 1°C of warming, the FishMIP ensemble projects a decrease in biomass of 2.84% [95% CI: 2.79; 2.9], against 4.22% [95% CI: 4.14; 4.3] for BOATS projections (Fig. 3a). In evaluating the impact of fishing of macrofauna biomass, we also contextualize BOATS results using global observational reconstructions based on stock assessment data³¹. At the global scale, BOATS simulations predict a slightly higher decline in biomass due to fisheries compared to global stock assessments; however, the uncertainty ranges overlap (Supplementary Table 5 and Supplementary Fig. 3). While using an ensemble of carbon export simulations with multiple MEMs would provide a more robust assessment under changing climate and fishing pressure, macrofauna-associated carbon export is not a requirement of the FishMIP protocol and is therefore not available for multiple models. Thus, our study only uses the BOATS to quantify marine macrofauna's carbon export by fecal pellets and carcasses. We acknowledge that structural differences between MEMs—such as using NPP or low-trophic-level biomass as the energy source—lead to uncertainties in the response of marine macrofauna biomass to

ocean warming³⁴. Even if the new generation of MEMs is increasingly consistent²², model disparities might lead to different responses of macrofauna carbon export to climate change. Consequently, the results presented here, based on a single model, should be considered as first-order estimates that provide a foundation to guide future work toward a more robust quantification of carbon export under climate change.

Global alteration of key macrofauna carbon areas (KMCAs)

Based on BOATS results, the cumulative impacts of fisheries and climate change (SSP 5–8.5) could cause a macrofauna biomass decline on $91\% \pm 8.3\%$ of the ocean surface by 2090 relative to the 1950s. On average, this decline would reach $-67\% \pm 8.5\%$, with the lowest decreases observed in the subtropical gyres (Fig. 4a–c). For carbon export, a lower but still large ocean surface area ($-82\% \pm 16\%$) is projected to experience a decline by 2090. In these areas, carbon export would decrease on average by $54\% \pm 13\%$, while in $18\% \pm 16\%$ of the ocean, export would increase by $82\% \pm 46\%$, compared to the 1950s (Fig. 4d–f). Increases in carbon export would mainly occur in the Atlantic Ocean, but also in the Indian Ocean and, to a smaller extent, in some oligotrophic parts of the Pacific Ocean (Fig. 4f), which contribute little to global export. However, these increases are uncertain due to large differences between NPP projections in CMIP6 ESMs under a high emission scenario (Supplementary Figs. 9 and 10)^{35,36}. This suggests that the positive effects of climate change on macrofauna carbon export may be overestimated in our study, and that the overall mean reduction in carbon export might also be underestimated. We then estimate the amount of carbon that would be sequestered in the ocean interior under contrasting scenarios using both transient and steady-

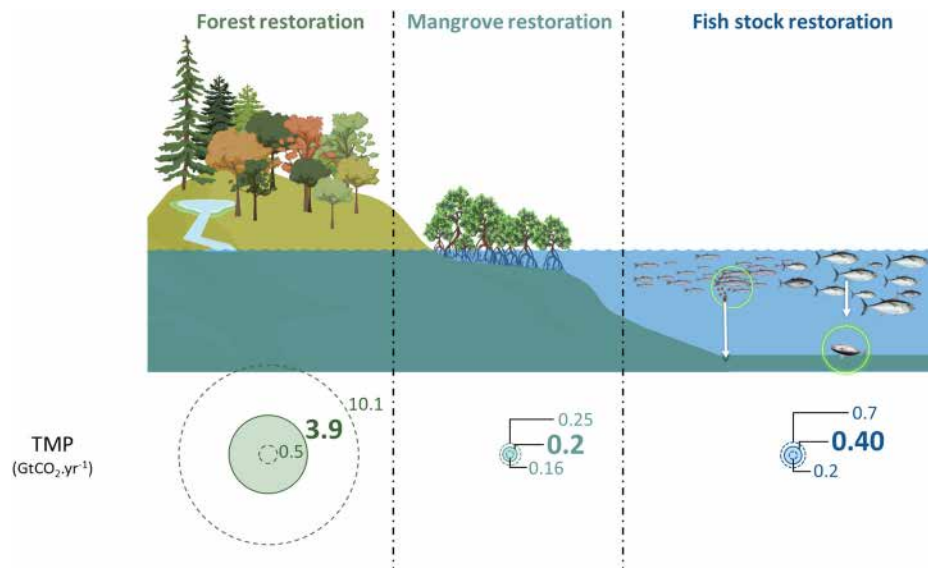


Fig. 6 | Comparison of the Technical Mitigation Potential (TMP, GtC yr⁻¹) between NbCS aiming to restore three major ecosystems: forests, mangroves, and macrofauna biomass. TMP estimates for forests and mangroves are from the

IPCC¹ and Hoegh-Guldberg et al.³⁸, respectively. Full circles represent the average value, inner and outer dashed circles represent the low and high estimates, respectively. Created in BioRender. Mariani, G. (2025) <https://BioRender.com/3rmmcyn>.

state simulations with the OCIM³⁰ (see “Methods” section). The transient simulations quantify how the ocean carbon inventory responds to changes in carbon export over the relatively short time frame up to year 2100. The steady-state simulations assume that transient changes will be sustained indefinitely over time, illustrating the potential maximum long-term effects of climate change and fisheries on carbon sequestration by macrofauna. Transient simulations show a reduction in macrofauna-driven carbon sequestration of $7.6\% \pm 2.3\%$ in 2090 compared to the 1950s sequestration of 128 ± 59 GtC (Supplementary Fig. 11). Steady-state simulations show that, if the 20th- and 21st-century declines in macrofauna carbon export were sustained indefinitely, the macrofauna-induced carbon sequestration would drop by $57\% \pm 16\%$ relative to 1950s levels (Supplementary Fig. 7). This suggests that fisheries and climate change could have long-term consequences on the stock of dissolved inorganic carbon generated by macrofauna in the ocean interior. It also illustrates that the impacts could be much smaller and more short-lived if fishing efforts and climate are returned relatively quickly to 1950s levels. Overall, the mean sequestration time of the macrofauna carbon is around 600 years and is not significantly affected by climate change and fishing pressure (see the “Materials and methods” section for further information on this calculation). Finally, our simulations suggest that fisheries have already impacted the distribution of marine macrofauna across the ocean, as well as the distribution of areas disproportionately contributing to carbon sequestration (Fig. 5a, b). In the 1950s, KMCA, defined as areas with both high (i.e., upper quartile) macrofauna biomass and high contribution to carbon sequestration (i.e., upper quartile, see “Methods” section) covered ~28 million km² and were mainly located in the Pacific Ocean (north and south American coasts), African Atlantic coasts, and in Australia’s northern waters (Fig. 5c). In the 2010s, the surface area of KMCA decreased to ~18 million km², suggesting that global change has already reduced the surface KMCA by 33.4% since the 1950s (Fig. 5c, d). The main erosion in KMCA took place in southern Australia and the west coasts of South America and Africa, and the shift of KMCA from the eastern equatorial Pacific to the western-central equatorial Pacific (Fig. 5c, d). However, given heterogeneous agreement between MEMs on the impact of climate on macrofauna biomass across regions²², the use of several MEMs might better reflect the spatial distribution of changes in carbon export. Anyhow, these rapid and broad-scale changes in KMCA highlight the strong impact of fisheries, stressing the

urgent need to include fishing pressure and carbon export in future MEM intercomparison efforts³⁷.

Oceanic refaunaation as an NbCS?

The recent IPBES-IPCC co-sponsored workshop on biodiversity and climate change suggests that climate change should “become part of the broader ecosystem-based approach to fisheries management, not only in terms of adaptation but also in terms of mitigation”¹⁶. Our results show that fisheries alter macrofauna carbon export both directly, by reducing macrofauna biomass and associated export, and indirectly, by altering size-dependent processes that control fecal pellet and carcass production. These findings show that restoring commercial macrofauna biomass could enhance carbon export and sequestration, thereby potentially serving as an NbCS. BOATS simulations suggest that, before the development of the fishing industry, marine macrofauna of commercial interest induced a carbon export of 0.23 ± 0.1 GtC yr⁻¹ (eq. to 0.8 GtCO₂ yr⁻¹). Given that fisheries have reduced this carbon export to 0.12 ± 0.037 GtC yr⁻¹ (eq. to 0.44 GtCO₂ yr⁻¹) in 2020, restoring macrofauna to a pristine level has a climate change mitigation potential of 0.11 GtC yr⁻¹ (eq. to 0.40 GtCO₂ yr⁻¹). This value can be considered as a technical mitigation potential (TMP, see IPCC¹), i.e., not considering social, economic, political, and environmental constraints that are likely to reduce this initial estimate. Although small compared to the TMP of other NbCS, such as forest restoration (3.9 [0.5 – 10.1] GtCO₂ yr⁻¹; IPCC¹), our estimate is of the same order of magnitude as that of mangrove restoration, and higher than the restoration of salt marshes (0.04 – 0.07 GtCO₂ yr⁻¹, Hoegh-Guldberg et al.³⁸) (Fig. 6). Another key but overlooked aspect of NbCS quality and importance is the time of sequestration³⁹, that is, the time after which the carbon sequestered in a given ecosystem returns to the atmosphere. Our results suggest that the mean sequestration time of the carbon produced by marine macrofauna is around 600 years. For comparison, in blue carbon ecosystems (mangrove, tidal marsh, seagrass), only 9% of the organic carbon buried will remain in the soil after 80–100 years upon burial⁴⁰. However, despite the long sequestration time of marine macrofauna carbon, macrofauna-based NbCS alone are unlikely to deliver meaningful climate change mitigation. Restoring marine macrofauna populations to pristine levels would sequester 0.4 GtCO₂ yr⁻¹ for 600 years, for a total of 240 GtCO₂, or roughly 6 years of total emissions (based on

annual emissions estimate of 42 GtCO₂ in 2024³³). Hence, the need for a drastic reduction in greenhouse gas emissions to limit the consequences of climate change¹. Overall, our findings suggest that macrofauna restoration would have relatively low mitigation potential but high durability, potentially offering a complementary pathway to terrestrial NbCS, on which we over-rely⁴¹, and where the permanency of carbon storage may be compromised by climate-related events^{6,7,42}. However, our first-order estimate should not be viewed as a sufficient justification to include macrofauna-related measures in the NbCS portfolio, given the substantial uncertainties and remaining knowledge gaps (see the section Caveats and limitations). Instead, our study is intended to stimulate further research into the relevance and feasibility of macrofauna restoration measures within the NbCS framework. On the other hand, other macrofauna-related measures, more focused on protection than restoration, seem to be more relevant and impactful. Indeed, mesopelagic fish, which are not taken into account here but whose biomass estimates range between 0.1 and 1.9 GtC^{43,44}, make a major contribution to the oceanic carbon cycle, exporting between 0.19 and 1 GtC every year^{12,45}. While several economic barriers are limiting the development of mesopelagic fisheries⁴⁶, these may be overcome to satisfy the growing demand for fishmeal^{47,48} without knowing the potential impact of such a development on carbon sequestration⁴⁹. Although NbCS related to marine macrofauna lack scientific readiness, those linked to mesopelagic fish appear to provide the strongest justification for implementing conservation measures⁵⁰ and applying the precautionary principle to the potential expansion of their exploitation⁵¹. In addition to restoration and protection efforts, fisheries could also be managed in a way that minimizes their effects on carbon export and sequestration in some critical places identified as KMCA. Indeed, given the higher metabolism of small fish, management strategies favoring small individuals might have higher carbon benefits than measures favoring large individuals. However, several other size- and age-dependent traits could make the benefits of larger individuals disproportionately more important than those of smaller ones. For example, the disproportionate reproductive advantages of large individuals could increase resilience to environmental and fisheries impacts⁵². Larger individuals are also known to respire at a slower mass-specific rate²⁴, making them more efficient at storing carbon in their living biomass than smaller ones⁵³. Therefore, if climate change mitigation and adaptation are the targets of future management goals, a balance must be found to enhance carbon export by smaller organisms while safeguarding the adaptation, carbon storage, and reproduction benefits of larger individuals.

Caveats and limitations

Significant knowledge gaps remain in understanding how marine macrofauna and their biogeochemical roles would respond to future human threats, as well as how management strategies targeting marine macrofauna can, in turn, impact climate change. Our analysis builds on simulations with the BOATS model, contextualized by comparison with available biomass data from the FishMIP ensemble²² and observational reconstructions of global commercial biomass³¹. Although these sources are globally consistent with one another for biomass predictions, our carbon export predictions with and without fishing are only based on an ensemble of ten BOATS simulations that account for parameter and scenario uncertainties. While parameter uncertainty can capture modulations related to the composition of marine macrofauna, it strongly relies on life histories representative of fish species. Thus, even though cephalopod catches are included in the model tuning procedure, aspects of their life history, such as their death after reproduction, which is known to inject a large amount of carbon in the deep ocean⁵⁴, are not well represented in the model. Given the range of biomass predictions from MEMs, addressing structural disparities between models will be crucial to enhance the reliability of future estimates of macrofauna's contribution to carbon export and

sequestration. Another major caveat of the BOATS model is that biomass production, and by extension, carbon export, is only influenced by bottom-up processes such as food availability^{26,27}. However, the depletion of marine macrofauna by fisheries (or conversely, its restoration by conservation efforts) can also influence lower trophic levels (e.g., phytoplankton and zooplankton) via top-down interactions such as nutrient regulation and predation⁵⁵. However, it remains unclear whether a reduction in macrofauna-mediated export by fisheries (or conversely, its increase by the restoration of commercial species) could be compensated by higher exports by non-targeted species, for example, mesopelagic fish or gelatinous zooplankton. Although not considered in this study, these indirect mechanisms may have a direct influence on the contribution of lower trophic levels to the carbon cycle, with potentially contrasting impacts on export and sequestration⁵⁶. Additionally, NbCS implementation in the marine realm can have negative consequences on the climate mitigation potential of other land-based measures. For example, restoration and management strategies targeting marine macrofauna through the reduction of catches may lead to an increase in the consumption of land-based proteins with a larger carbon footprint, such as beef and pork⁵⁷. Moreover, restoration efforts may affect atmospheric CO₂ levels, potentially altering the mitigation potential of terrestrial carbon sinks⁵⁸, as seen in oceanic afforestation studies⁵⁹. Incorporating these important feedback loops into cross-sectoral models is therefore crucial for more realistic estimates of the mitigation potential of marine macrofauna-related NbCS. Finally, to be considered as an NbCS, oceanic refauna should have a direct impact on atmospheric CO₂ concentrations. However, unlike terrestrial NbCS, oceanic NbCS does not directly remove CO₂ from the atmosphere. This removal only occurs when the seawater CO₂ equilibrates with the atmosphere, a process influenced by factors including sea surface water residence time and depth of the mixed layer^{60–62}. Consequently, in oceanic areas where this balancing process is inefficient, the TMP of oceanic refauna might be overestimated, and the true impact of these measures on atmospheric CO₂ concentration remains to be quantified. In addition, the amount of CO₂ removed from the atmosphere must also be verified to be considered a high-quality offset³⁹. Yet, due to the difficulties of attributing changes in air–sea CO₂ fluxes to a measure of macrofauna restoration^{61,63}, approaches to evaluate the benefits of NbCS, i.e., monitoring, reporting, and verification (MRV), remain difficult to apply in the case of ocean-related NbCS. As a result, these potential marine NbCS cannot be included in current offsetting schemes, and a robust MRV system able to monitor additional CO₂ uptake would have to be developed⁶⁴.

Concluding remarks

Large transformations are needed to reduce the impact of every sector contributing to the dual climate and biodiversity crisis. Achieving such transformations in the marine sector requires more than achieving solely the maximum sustainable yield to supply the growing demand for blue food⁶⁵. Acknowledging the integral roles of marine macrofauna in the carbon cycle and their vulnerability to fisheries can be a way to foster the implementation of impactful management strategies that feed people without imperiling biodiversity and climate objectives⁶⁶. Here, global biomass reconstructions of commercial species suggest that historical fishing pressure has significantly reduced the capacity of marine macrofauna to export and sequester carbon. The historical impact of fisheries far exceeds that projected to occur due to ocean warming in the 21st century, and suggests that the restoration of commercial macrofauna could be a candidate to qualify as a novel NbCS. However, major sources of uncertainty persist regarding the climate impact of marine macrofauna restoration, and the ability to monitor, report, and verify its effects on atmospheric CO₂ concentrations. Reducing these uncertainties and filling these

knowledge gaps requires an approach that combines science, finance, and governance, while drawing lessons from past mistakes in other NbCS measures^{39,67,68}, to avoid undesirable outcomes on climate, biodiversity, and society.

Methods

Model scenarios

To explore the impact of global change (fishing and climate change) on carbon export and sequestration by marine macrofauna of commercial interest, we force BOATS with two contrasting scenarios of climate change: the respect of the Paris Agreement (SSP 1–2.6) and the business-as-usual scenarios (SSP 5–8.5). Two variables were used to force the model of biomass prediction (BOATS, see the next section), the NPP and the SST. In BOATS, following macroecological theory, NPP drives the accumulation of biomass in marine macrofauna based on factors such as trophic efficiency, predator-prey mass ratio, and phytoplankton size, while temperature affects physiological rates, including growth, mortality, and reproduction^{24,26}. These two variables were obtained from two ESMs from the Couple Model Intercomparison Project 6 (CMIP6), namely the Geophysical Fluid Dynamics Laboratory (GFDL) and the Institut Pierre-Simon Laplace (IPSL). They cover the historical period 1950–2014 and future projections from 2015 to 2100. To explore the cumulative impact of climate change and fisheries, we also ran climate change scenarios together with contrasting scenarios of fishing effort: one without exploitation and another one where exploitation evolves dynamically to match the historical harvest dynamic until 2014, and where fishing effort is kept constant in the future until 2100. This protocol for simulations is the protocol of the Fisheries and MEM Intercomparison Project (FishMIP) for the ISIMIP3b²⁹. These simulations were contributed, along with other MEMs, to the intercomparison of global fish biomass projections²². To compare BOATS biomass outputs in the fishing scenario, we also used global reconstruction data based on stock assessments from Worm and Branch³¹.

Alongside BOATS, to acknowledge structural and parameter differences between MEMs in simulating the impact of climate change on marine biomass²², we also used simulation outputs of a set of five other MEMs (Apecosm, DBPM, EcoOcean, FEISTY, and ZooMSS), referred to as “FishMIP simulations” in the main text. The simulations and model characteristics are described in the global fish biomass projection intercomparison by Tittensor et al.²² (see Supplementary Table 4 for model references and acknowledgments of the contributing modeling groups).

Description of the model BOATS

We used the BOATS model (Carozza et al.^{26,27} to estimate the change in biomass of marine macrofauna from 10 g to 100 kg targeted by fisheries (hereafter called macrofauna for simplicity). The main ecological model parameters and variables are listed in the Supplementary Tables 1–3. Macrofauna biomass is divided into three species groups k , the small, the medium, and the large species groups, and each group is itself divided into size classes. For each group, the life history of an individual starts in the first size class (10 g) and can grow until it reaches its asymptotic mass, so 0.3 kg, 8.5 kg, and 100 kg for the small, medium, and large species, respectively. The main model equation that estimates the variation through time (t) of macrofauna biomass per mass class m in each group k , $f_k(m, t)$ corresponds to:

$$\frac{\partial}{\partial t} f_k(m, t) = \frac{\partial}{\partial m} \gamma_{S,k}(m, t) \bullet f_k(m, t) + \frac{\gamma_{S,k}(m, t) \bullet f_k(m, t)}{m} - [\Lambda_k(m) + \Lambda_F(m, t)] \bullet f_k(m, t) \quad (1)$$

The first two terms on the right-hand side represent, respectively, the somatic growth of an individual across size classes, at a rate γ_S , and the accumulation of macrofauna biomass within the same size class. The

third and last term of the equation represents losses from natural mortality that occur at a rate Λ_k and from fishing mortality that occurs at a rate Λ_F . Both rates vary with time, with the average temperature in the upper ocean (top 75 m) and/or the vertically integrated NPP. The somatic growth rate ($\gamma_{S,k}$) corresponds to the net energy input needed for growth (somatic + reproduction) ($\xi_{I,k}$) minus the fraction of energy allocated to reproduction ($\gamma_{R,k}$):

$$\gamma_{S,k} = \xi_{I,k} - \gamma_{R,k} \quad (2)$$

Here, $\xi_{I,k}$ is the minimum value between the theoretical maximum temperature-dependent growth rate in *ad libitum* food conditions derived from the assumption of a Von Bertalanffy growth ($\xi_{VB,k}$), and a growth rate limited by NPP ($\xi_{P,k}$), so based on the amount of energy available from primary production. This means that the net growth rate cannot exceed the biologically determined maximum rate, even under high NPP:

$$\xi_{I,k} = \min(\xi_{VB,k}, \xi_{P,k}) \quad (3)$$

with

$$\xi_{VB,k} = A \bullet m^b - k_a \bullet m \quad (4)$$

where $A = A_0 \bullet a_A(T)$, A_0 being the allometric growth constant⁶⁹, modulated by $a_A(T)$ the van't Hoff-Arrhenius exponential temperature dependence of growth, $a_A(T) = \exp\left(\frac{\omega_{a,A}}{k_B} \bullet \left(\frac{1}{T_{ref}} - \frac{1}{T}\right)\right)$, with $\omega_{a,A}$ the growth activation energy of metabolism, k_B the Boltzmann constant while T and T_{ref} are the local temperature and a reference temperature, respectively. The term $k_a \bullet m$ accounts for the energy dissipation through activity, it is also proportional to $a_A(T)$ (see Carozza et al.²⁶). When primary production is limiting:

$$\xi_{P,k} = \frac{\phi_C \bullet \pi \bullet m}{f_k} \quad (5)$$

$$\pi = \frac{\Pi_\psi}{m_\psi} \bullet \left(\frac{m}{m_\psi}\right)^{\tau-1} \quad (6)$$

where Π_ψ is the vertically integrated NPP, τ is the trophic scaling exponent (i.e., how efficiently energy is transferred through the trophic web), and m_ψ is the representative size of phytoplankton at which NPP takes place, estimated as the geometric mean of phytoplanktonic groups mass, $m_\psi = m_L^{\Phi_L(t)} + m_S^{1-\Phi_L(t)}$, Φ_L being the proportion of large cells and m the mass of large and small cells (as in Dunne, et al.⁷⁰).

Finally, the energy allocated to reproduction ($\gamma_{R,k}$) corresponds to the fraction (ϕ_k) of net energy input ($\xi_{I,k}$) allocated to reproduction:

$$\gamma_{R,k} = \phi_k \bullet \xi_{I,k} \quad (7)$$

where ϕ_k is the mass-dependent fraction of input energy that is allocated to reproduction. Rewriting Eq. (2) provides:

$$\gamma_{S,k} = (1 - \phi_k) \bullet \xi_{I,k} \quad (8)$$

and assuming that $\gamma_{R,k}$ is proportional to mass and scales with a size-dependent rate $s_k(m)$, so that $\gamma_{R,k} = k_r^{\max} \bullet s_k \bullet m$, we can estimate $\phi_k(m)$ as:

$$\phi_k = \frac{k_r^{\max} \bullet s_k \bullet m}{\xi_{I,k}}; \text{ with } \xi_{I,k} = \xi_{VB,k} \quad (9)$$

Where k_r^{\max} , the normalizing constant, is estimated by solving the equation $\phi_k(m_\infty) = 1$, so all energy input goes to reproduction when m_∞ is reached:

$$k_r^{\max} = \frac{\xi_{VB,k}(m_{\infty,k})}{s_k(m_{\infty,k}) \bullet m_{\infty,k}} \quad (10)$$

Thus, Eq. (8) can be written as:

$$\gamma_{S,k} = \left(1 - \frac{\xi_{VB,k}(m_{\infty,k}) \bullet s_k \bullet m}{s_k(m_{\infty,k}) \bullet m_{\infty,k} \bullet \xi_{VB,k}}\right) \bullet \min(\xi_{VB,k}, \xi_{P,k}) \quad (11)$$

For the mortality term in Eq. (1), Λ_F corresponds to the fishing mortality rate. It equals:

$$\Lambda_{F,k}(m, t) = q_k(t) \bullet \sigma_k(m) \bullet E_k(t) \quad (12)$$

It represents the catch of macrofauna group k at the size m , and is a function of the catchability q , a measure of the technological efficiency of fishing gear to capture macrofauna biomass, the selectivity function $\sigma(m)$, which varies between 0 and 1 and expresses the intrinsic ability of a given gear to target a given size class m , and the fishing effort E .

In the simulations without fishing, there is no fishing effort E and no fishing mortality $\Lambda_{F,k}$. With fishing, over the historical period (1950–2014), fishing effort evolves dynamically under an open-access dynamic proportional to the local net profit for the difference between fishing revenues and costs²⁷. Effort is held constant at the 2015 level for projections to the year 2100. By design, BOATS is tuned to reproduce key aspects of global fisheries catch, including total catch, size structure of the catch, catch-to-biomass ratio, and maximum catch potential of large marine ecosystems (LME), when forced with observed satellite-based NPP and temperature²⁹. Here, we use the same model configuration and parameters, but force the model with historical ESM simulations and future projections. To account for parameter uncertainty, an ensemble of 10,000 simulations at the LME level was conducted during model tuning, from which five representative parameter sets were selected (see Supplementary Table 3)^{27,28}. Here, each simulation is replicated five times using the five parameter sets, resulting in a total of 20 simulations: 5 parameter sets \times 2 ESMs (GFLD and IPSL) \times with or without fishing. The model equations are solved numerically with a monthly time-step on a global $1^\circ \times 1^\circ$ grid, for 3 species groups (small, medium, and large asymptotic size), with a discretisation of the biomass size spectrum into 50 size classes. We report the mean and standard deviation of the five replicate parameter sets for each combination of ESM and fishing scenario.

Modeling carcass production

In BOATS, the natural mortality rate (Λ_k) represents all forms of natural mortality, including predation and non-predation mortality:

$$\Lambda_k = \Lambda_{pred} + \Lambda_{non-pred} \quad (13)$$

In BOATS, Λ_k depends on temperature, mass, and asymptotic mass and is derived from Gislason et al.⁷¹, where all mortality causes are nested in a general formula, used for each species group k :

$$\Lambda_k = \lambda(T) \bullet m^{-h} \bullet m_{\infty}^{h+b-1} \quad (14)$$

where m , m_∞ , h , and b are respectively the mass, the asymptotic mass, the allometric mortality scaling exponent, and the allometric growth scaling exponent. $\lambda(T)$ is the temperature-dependent term

estimated as:

$$\lambda(T) = \frac{e^{\zeta_1} \bullet A_0 \bullet a_\lambda(T)}{3} \quad (15)$$

with ζ_1 a mortality constant estimated from Gislason et al.⁷¹, A_0 is the allometric growth constant from Andersen and Beyer⁶⁹ and $a_\lambda(T) = \exp\left(\frac{\omega_{a,\lambda}}{k_B} \bullet \left(\frac{1}{T_{ref}} - \frac{1}{T}\right)\right)$ the van't Hoff-Arrhenius exponential function for mortality.

The dead biomass of a group k ($B_{Dead,k}$) therefore corresponds to the portion of the biomass in that group (f_k) that dies naturally:

$$B_{Dead,k} = \Lambda_k \bullet f_k \quad (16)$$

To estimate the proportion of that biomass that sinks to the deep-sea floor (i.e., the biomass not dead from predation), we estimated the contribution of $\Lambda_{non-pred,k}$ to the total mortality Λ_k , noted $\Delta_{contrib,k}$, as:

$$\Delta_{contrib,k} = \frac{\Lambda_{non-pred,k}}{\Lambda_k} \quad (17)$$

We used the formula in Rogers, et al.⁷² to estimate $\Lambda_{non-pred,k}$, while adding a temperature dependency term $a_\lambda(T)$:

$$\Lambda_{non-pred,k} = \left(\mu_R \bullet m^{-\beta_R} + \mu_S \bullet \left(\frac{m}{m_S}\right)^{\beta_S}\right) \bullet a_\lambda(T) \quad (18)$$

Here, the first term ($\mu_R \bullet m^{-\beta_R}$) corresponds to the extrinsic mortality, so mortality mainly from starvation, which decreases exponentially with an increase in body mass (m). The second term ($\mu_S \bullet \left(\frac{m}{m_S}\right)^{\beta_S}$) mimics the mortality from senescence, so that larger individuals have a higher probability of dying once the mass at senescence (m_S) is reached. The addition of both terms leads to the well-known U-shaped mortality function.

Although this function is derived from a model for coral-reef fish, U-shaped age-dependent mortality curves are well-documented for several species across the tree of life, including fish⁷³. U-shaped age-dependent mortality functions are also used to model offshore species population dynamics such as tuna and tuna-like species (see Lehodey et al.⁷⁴ with an application to carcass production in Mouillot et al.²³). Although refining the parametrization of this function with species-specific data would further improve the accuracy of our estimate, the current knowledge, as well as the structure of the BOATS model, does not allow us to use a species- or group-specific (inshore vs offshore species) formula. We believe our approach, using a general U-shaped function, provides an ecologically grounded first-order estimate of carcass production across diverse fish groups.

The total dead biomass that sinks to the deep-sea floor ($B_{sink,k}$) therefore equals to:

$$B_{sink,k} = \Delta_{contrib,k} \bullet B_{Dead,k} \quad (19)$$

For the largest macrofauna only (i.e., size classes 50 of group 3) (Supplementary Figs. 4–6), it happens that the contribution of the non-predation mortality to the total mortality exceeds 1. In that case, we estimated that these organisms cannot die from predation but only from senescence, by limiting the value to 1.

Modeling fecal pellet production

We estimated carbon loss by macrofauna (respiration + fecal pellets) at the individual level ($C_{i,k}$) by first computing total energy input or gross ingestion (ξ_{TOT}), i.e., the energy needed for reproduction, growth, plus loss¹⁹. ξ_{TOT} is estimated using the net biomass production ξ_i (see Eq. (3)), divided by the assimilation efficiency (α):

$$\xi_{TOT} = \frac{\xi_i}{\alpha} \quad (20)$$

As carbon loss corresponds to the difference between total ingestion (ξ_{TOT}) and the part used for growth and reproduction ($\xi_{i,k}$), $C_{i,k}$ equals to:

$$C_{i,k} = \xi_{TOT} - \xi_{i,k} = \frac{\xi_{i,k}}{\alpha} - \xi_{i,k} \quad (21)$$

Factorizing Eq. (21) leads to:

$$C_{i,k} = \frac{1-\alpha}{\alpha} \bullet \xi_{i,k} \quad (22)$$

To scale carbon loss (respiration + fecal pellets) to the entire population (C_{total}), we integrated the individual carbon loss $C_{i,k}$ over the entire size spectrum for each species group k , and summed it:

$$C_{total} = \sum_k C_k \quad (23)$$

Where C_k , so the entire carbon loss from group k equals:

$$C_k = \int_{m_0}^{m_{\infty,k}} C_{i,k}(m) \bullet n_k(m) dm \quad (24)$$

Where $n_k(m)$ corresponds to the abundance of macrofauna in a given group k and size class, $n_k(m) = \frac{f_k(m, t)}{m}$.

As in Bianchi et al.¹⁹, we assume that about $\phi_E = 20\%$ of the biomass cycling rate is returned to the environment as fecal pellets, the remaining 80% being respired.

Modeling carbon export from fecal pellets and carcasses

We model the export of fecal pellets and carcass at depth z (FFP_z) in each cell using an exponential function⁷⁵ with a temperature-dependent microbial remineralization rate (k_{remin}) and a sinking speed of macrofauna fecal pellets or carcass (W_{sink}). Once reaching the bottom of the ocean, we considered that the carbon is entirely remineralized in the last layer and is not buried in the sediment.

$$FFP_{z+1} = FFP_z \times e^{\left(\frac{k_{remin}}{W_{sink}} \times ((z+1)-z) \right)} \quad (25)$$

To take into account the impact of climate change on the microbial activity (remineralization), we used a temperature coefficient (Q_{10}) of 2, so the microbial activity increases by a factor of 2 for each 10 °C increase, so that k_{remin} equals:

$$k_{remin} = k_1 \times Q_{10}^{\frac{T_2 - T_1}{10}} \quad (26)$$

where k_1 is the initial remineralization coefficient at a reference temperature T_1 , and T_2 is the temperature in each cell at a given depth. The parameter W_{sink} is set to 787 m d⁻¹ and 1150 m d⁻¹ for fecal pellets and carcass, respectively^{12,76}. We assumed that all fecal pellets were produced above the euphotic zone, at a depth z of $z_{eu} = 75$ m. As the temperature of the ocean varies with depth, we divided the ocean into coarse layers, 0–200 m, 200–500 m, 500–1000 m, 1000–2000 m, and

2000 m to the bottom, and used the temperature fields from the CMIP6 GFDL and IPSL model forcings. Since there is a strong drift in potential temperature in the two last layers, we identified and removed the trend (linear detrending) using preindustrial control simulations. Finally, we ran the export model in a three dimensional ocean of dimensions 180 × 360 × 24, the last dimension corresponding to the 24 depth layers used later in the OCIM (next section).

Modeling carbon sequestration

We estimate the amount of carbon stored in the ocean interior by marine macrofauna using the OCIM³⁰. The spatial resolution of the OCIM is 2° horizontally with 24 vertical depth layers. We use it here to track DIC injected (C_{inj}) by carbon remineralization in the interior ocean. C_{inj} was estimated using the result of Eq. (25) for each depth layer as:

$$C_{inj_z} = FFP_z - FFP_{z+1} \quad (27)$$

The tracer equation used to estimate the concentration and distribution of the injected DIC (C) corresponds to:

$$\frac{dC}{dt} = T * C + C_{inj} \quad (28)$$

Here, T corresponds to the transport matrix operator that accounts for ocean currents (i.e., advection-diffusion matrix), C is the concentration of DIC, and C_{inj} is the source of DIC from the remineralization of macrofauna-derived organic carbon converted in $\mu\text{mol/kg/yr}$. For simplicity, we assume a boundary condition of $C=0$ at the sea-surface, which assumes instantaneous air-sea equilibration⁶². Given that a new steady-state resulting from changes in carbon export will be reached in several centuries (~1000 years), we ran both transient and steady-state simulations. Transient simulations illustrate the real-time impact of changing exports on carbon sequestration, while steady-state simulations assume that transient changes will be sustained indefinitely over time, illustrating the potential maximum long-term effects of climate change and fisheries on carbon sequestration by macrofauna. An initial pre-industrial baseline was found by solving Eq. (27) at steady-state and using C_{inj} for 1950. Then, a transient simulation with yearly changing export was performed using the backward Euler method, starting at 1950 and ending in 2100. Finally, we found another steady-state assuming that the C_{inj} value for 2100 extends indefinitely into the future. We obtained the total carbon sequestered by macrofauna in the ocean interior by globally integrating C to obtain a value of carbon sequestration (C_{seq}) in GtC. The time of sequestration (in years) was obtained by dividing C_{seq} by the globally integrated carbon export (in GtC yr⁻¹). Finally, we calculated the carbon sequestration origin, or regions where carbon sequestered by macrofauna in the ocean interior comes from, as the product of carbon injected at each depth and the mean sequestration time at that depth, also known as the mean first-passage time (e.g., Siegel et al.⁷⁷, Primeau⁷⁸). The OCIM was run on MATLAB.

Estimation of KMCAs

KMCAs are defined using an upper quartile method as areas where both the commercial macrofauna biomass and their contribution to carbon sequestration are high (i.e., value of biomass and contribution to carbon sequestration in the upper quartile). To quantify the impact of fishing and climate change on the spatial distribution of the KBCA, we estimated the spatial distribution of the KBCA for two decades: in the 1950s in a scenario without fishing, and the 2010' in a scenario with historical fishing. All analyses were done in the R statistical computing

environment (version 4.1.0)⁷⁹. All outputs are available at Mariani et al.⁸⁰.

Reporting summary

Further information on research design is available in the Nature Portfolio Reporting Summary linked to this article.

Data availability

All data needed to reproduce the figures and analysis are available online at Zedono: <https://doi.org/10.5281/zenodo.17085415>⁸⁰.

Code availability

The code needed to reproduce the figures and analysis in the manuscript is available online at Zedono: <https://doi.org/10.5281/zenodo.17085415>⁸⁰. Scripts for the BOATS model and processed forcings for the simulations presented in the manuscript are available at <https://zenodo.org/records/16648800>.

References

- IPCC. *Climate Change 2022: Mitigation of Climate Change. Contribution of Working Group III to the Sixth Assessment Report of the Intergovernmental Panel on Climate Change* (Cambridge University Press, Cambridge, 2022).
- Seddon, N. Harnessing the potential of nature-based solutions for mitigating and adapting to climate change. *Science* **376**, 1410–1416 (2022).
- Griscom, B. W. et al. Natural climate solutions. *PNAS* **114**, 11645–11650 (2017).
- Roe, S. et al. Land-based measures to mitigate climate change: potential and feasibility by country. *Glob. Chang Biol.* **27**, 6025–6058 (2021).
- Anderegg, W. R. L. et al. Climate-driven risks to the climate mitigation potential of forests. *Science* **368**, eaaz7005 (2020).
- Hammond, W. M. et al. Global field observations of tree die-off reveal hotter-drought fingerprint for Earth's forests. *Nat. Comm.* **13**, 1761 (2022).
- Burton, C. et al. Global burned area increasingly explained by climate change. *Nat. Clim. Chang.* **14**, 1186–1192 (2024).
- Byrne, B. et al. Carbon emissions from the 2023 Canadian wildfires. *Nature* <https://doi.org/10.1038/s41586-024-07878-z> (2024).
- MacCarthy, J., Tyukavina, A., Weisse, M. J., Harris, N. & Glen, E. Extreme wildfires in Canada and their contribution to global loss in tree cover and carbon emissions in 2023. *Glob. Chang Biol.* **30**, e17392 (2024).
- Doney, S. C. et al. Observational and numerical modeling constraints on the global ocean biological carbon pump. *Glob. Biogeochem. Cycles* **38**, e2024GB008156 (2024).
- Nowicki, M., DeVries, T. & Siegel, D. A. Quantifying the carbon export and sequestration pathways of the ocean's biological carbon pump. *Global Biogeochem. Cycles*. <https://doi.org/10.1029/2021gb007083> (2022).
- Pinti, J. et al. Model estimates of metazoans' contributions to the biological carbon pump. *Biogeosciences* **20**, 997–1009 (2023).
- Saba, G. K. et al. Toward a better understanding of fish-based contribution to ocean carbon flux. *Limnol. Oceanogr.* <https://doi.org/10.1002/lno.11709> (2021).
- Cavan, E. L. & Hill, S. L. Commercial fishery disturbance of the global ocean biological carbon sink. *Glob. Chang Biol.* **28**, 1212–1221 (2022).
- Henson, S. A. et al. Uncertain response of ocean biological carbon export in a changing world. *Nat. Geosci.* **15**, 248–254 (2022).
- Pörtner, H. O. et al. IPBES-IPCC co-sponsored workshop report on biodiversity and climate change; IPBES and IPCC. *IPBES Secretar.* <https://doi.org/10.5281/zenodo.4782538> (2021).
- UNEP. Nature-based Solutions for Climate Change Mitigation (UNEP, 2021).
- Letessier, T. B. et al. Divergent responses of pelagic and benthic fish body-size structure to remoteness and protection from humans. *Science* **383**, 976–982 (2024).
- Bianchi, D., Carozza David, A., Galbraith Eric, D., Guiet, J. & DeVries, T. Estimating global biomass and biogeochemical cycling of marine fish with and without fishing. *Sci. Adv.* **7**, eabd7554 (2021).
- Free, C. M. et al. Impacts of historical warming on marine fisheries production. *Science* **363**, 979–983 (2019).
- Lotze, H. K. et al. Global ensemble projections reveal trophic amplification of ocean biomass declines with climate change. *Proc. Natl. Acad. Sci. USA* **116**, 12907–12912 (2019).
- Tittensor, D. P. et al. Next-generation ensemble projections reveal higher climate risks for marine ecosystems. *Nat. Clim. Chang* **11**, 973–981 (2021).
- Mouillot, D. et al. Industrial fisheries have reversed the carbon sequestration by tuna carcasses into emissions. *Glob. Chang Biol.* <https://doi.org/10.1111/gcb.16823> (2023).
- Brown, J. H., Gillooly, J. F., Allen, A. P., Savage, V. M. & West, G. B. Toward a metabolic theory of ecology. *Ecology* **85**, 1771–1789 (2004).
- van Rijn, I., Buba, Y., DeLong, J., Kiflawi, M. & Belmaker, J. Large but uneven reduction in fish size across species in relation to changing sea temperatures. *Glob. Chang Biol.* **23**, 3667–3674 (2017).
- Carozza, D. A., Bianchi, D. & Galbraith, E. D. The ecological module of BOATS-1.0: a bioenergetically constrained model of marine upper trophic levels suitable for studies of fisheries and ocean biogeochemistry. *Geosci. Model Dev.* **9**, 1545–1565 (2016).
- Carozza, D. A., Bianchi, D. & Galbraith, E. D. Formulation, general features and global calibration of a bioenergetically-constrained fishery model. *PLOS ONE* **12**, e0169763 (2017).
- Galbraith, E. D., Carozza, D. A. & Bianchi, D. A coupled human-Earth model perspective on long-term trends in the global marine fishery. *Nat. Comm.* **8**, 14884 (2017).
- Tittensor, D. P. et al. A protocol for the intercomparison of marine fishery and ecosystem models: Fish-MIP v1.0. *Geosci. Model Dev.* **11**, 1421–1442 (2018).
- DeVries, T. The oceanic anthropogenic CO₂ sink: storage, air-sea fluxes, and transports over the industrial era. *Glob. Biogeochem. Cycles* **28**, 631–647 (2014).
- Worm, B. & Branch, T. A. The future of fish. *TREE* **27**, 594–599 (2012).
- Lindmark, M., Ohlberger, J. & Gårdmark, A. Optimum growth temperature declines with body size within fish species. *Glob. Chang Biol.* **28**, 2259–2271 (2022).
- Forster, P. M. et al. Indicators of Global Climate Change 2024: annual update of key indicators of the state of the climate system and human influence. *Earth Syst. Sci. Data* **17**, 2641–2680 (2025).
- Heneghan, R. F. et al. Disentangling diverse responses to climate change among global marine ecosystem models. *Prog. Oceanogr.* **198**, 102659 (2021).
- Kwiatkowski, L. et al. Twenty-first century ocean warming, acidification, deoxygenation, and upper-ocean nutrient and primary production decline from CMIP6 model projections. *Biogeosciences* **17**, 3439–3470 (2020).
- Bopp, L. et al. Diazotrophy as a key driver of the response of marine net primary productivity to climate change. *Biogeosciences* **19**, 4267–4285 (2022).
- Maur, O. et al. *The Ocean System Pathways (OSPs): a New Scenario and Simulation Framework to Investigate the Future of the World Fisheries* (ESS Open Archive, 2024).
- Hoegh-Guldberg, O. et al. *The Ocean as a Solution to Climate Change: Five Opportunities for Action* (World Resources Institute, 2019).

39. Boyd, P., Bach, L., Holden, R. & Turney, C. Carbon offsets aren't helping the planet—four ways to fix them. *Nature* **620**, 947–949 (2023).
40. Piñeiro-Juncal, N. et al. Soil organic carbon depth profiles and centennial and millennial decay rates in tidal marsh, mangrove and seagrass blue carbon ecosystems. *Commun. Earth Environ.* **6**, 504 (2025).
41. Dooley, K., Christiansen, K. L., Lund, J. F., Carton, W. & Self, A. Over-reliance on land for carbon dioxide removal in net-zero climate pledges. *Nat. Comm.* **15**, 9118 (2024).
42. Robbins, Z. J. et al. Warming increased bark beetle-induced tree mortality by 30% during an extreme drought in California. *Glob. Chang. Biol.* **28**, 509–523 (2022).
43. Pauly, D. et al. The biology of mesopelagic fishes and their catches (1950–2018) by commercial and experimental fisheries. *J. Mar. Sci. Eng.* **9**, 1057 (2021).
44. Irigoien, X. et al. Large mesopelagic fishes biomass and trophic efficiency in the open ocean. *Nat. Comm.* **5**, 3271 (2014).
45. Aumont, O., Maury, O., Lefort, S. & Bopp, L. Evaluating the potential impacts of the diurnal vertical migration by marine organisms on marine biogeochemistry. *Glob. Biogeochem. Cycles* **32**, 1622–1643 (2018).
46. Oostdijk, M., Elsler, L. G., Ramírez-Monsalve, P., Orach, K. & Wisz, M. S. Governing open ocean and fish carbon: perspectives and opportunities. *Front. Mar. Sci.* <https://doi.org/10.3389/fmars.2022.764609> (2022).
47. Kourantidou, M. & Jin, D. Mesopelagic–epipelagic fish nexus in viability and feasibility of commercial-scale mesopelagic fisheries. *Nat. Resour. Model.* **35**, e12350 (2022).
48. FAO. *The State of World Fisheries and Aquaculture 2022. Towards blue transformation* (FAO, Rome, 2022).
49. Schadeberg, A., Kraan, M., Groeneveld, R., Trilling, D. & Bush, S. Science governs the future of the mesopelagic zone. *npj Ocean Sustain.* **2**, 2 (2023).
50. Collins, J. R. et al. The biogeochemistry of natural climate solutions based on fish, fisheries, and marine mammals: a review of current evidence, research needs, and critical assessment of readiness. *Glob. Biogeochem. Cycles* **39**, e2024GB008393 (2025).
51. Oostdijk, M. et al. Modeling fisheries and carbon sequestration ecosystem services under deep uncertainty in the ocean twilight zone. *Ambio* **53**, 1632–1648 (2024).
52. Barneche, D. R., Robertson, D. R., White, C. R. & Marshall, D. J. Fish reproductive-energy output increases disproportionately with body size. *Science* **360**, 642–645 (2018).
53. Falciani, J. E., Grigoratou, M. & Pershing, A. J. Optimizing fisheries for blue carbon management: why size matters. *Limnol. Oceanogr.* **67**, S171–S179 (2022).
54. Ottmann, D., Daniël van Denderen, P., Visser, A. & Andersen, K. H. Impact of increased fishing on long-term sequestration of carbon by cephalopods. *Curr. Biol.* **34**, R526–R527 (2024).
55. Lynam, C. P. et al. Interaction between top–down and bottom-up control in marine food webs. *PNAS* **114**, 1952–1957 (2017).
56. Dupont, L. et al. High trophic level feedbacks on global ocean carbon uptake and marine ecosystem dynamics under climate change. *Glob. Chang. Biol.* **29**, 1545–1556 (2023).
57. Poore, J. & Nemecek, T. Reducing food's environmental impacts through producers and consumers. *Science* **360**, 987–992 (2018).
58. Keller, D. P. et al. The carbon dioxide removal model inter-comparison project (CDRMP): rationale and experimental protocol for CMIP6. *Geosci. Model Dev.* **11**, 1133–1160 (2018).
59. Wu, J., Keller, D. P. & Oschlies, A. Carbon dioxide removal via macroalgae open-ocean mariculture and sinking: an Earth system modeling study. *Earth Syst. Dynam.* **14**, 185–221 (2023).
60. Jones, D. C., Ito, T., Takano, Y. & Hsu, W.-C. Spatial and seasonal variability of the air–sea equilibration timescale of carbon dioxide. *Glob. Biogeochem. Cycles* **28**, 1163–1178 (2014).
61. Bach, L. T., Ho, D. T., Boyd, P. W. & Tyka, M. D. Toward a consensus framework to evaluate air–sea CO₂ equilibration for marine CO₂ removal. *Limnol. Oceanogr. Lett.* <https://doi.org/10.1002/lol2.10330> (2023).
62. Nowicki, M., DeVries, T. & Siegel, D. A. The influence of air–sea CO₂ disequilibrium on carbon sequestration by the ocean's biological pump. *Glob. Biogeochem. Cycles* **38**, e2023GB007880 (2024).
63. Boyd, P. W., Gattuso, J. P., Hurd, C. L. & Williamson, P. Limited understanding of basic ocean processes is hindering progress in marine carbon dioxide removal. *Environ. Res. Lett.* **19**, 061002 (2024).
64. Ho, D. T. & Bopp, L. Marine carbon dioxide removal may be a future climate solution. *Dialogues Clim. Change* **1**, 56–62 (2024).
65. Jacquet, J. & Pauly, D. Reimagining sustainable fisheries. *PLoS Biol.* **20**, e3001829 (2022).
66. Martin, A. H. & Scheffold, M. I. E. & O'Leary, B. C. Changing the narrative and perspective surrounding marine fish. *Mar. Policy* **156**, 105806 (2023).
67. West, T. A. P. et al. Action needed to make carbon offsets from forest conservation work for climate change mitigation. *Science* **381**, 873–877 (2023).
68. Cullenward, D., Badgley, G. & Chay, F. Carbon offsets are incompatible with the Paris agreement. *One Earth* **6**, 1085–1088 (2023).
69. Andersen, K. H. & Beyer, J. E. Size structure, not metabolic scaling rules, determines fisheries reference points. *Fish Fish* **16**, 1–22 (2015).
70. Dunne, J. P., Armstrong, R. A., Gnanadesikan, A. & Sarmiento, J. L. Empirical and mechanistic models for the particle export ratio. *Global Biogeochem. Cycles*. <https://doi.org/10.1029/2004GB002390> (2005).
71. Gislason, H., Daan, N., Rice, J. C. & Pope, J. G. Size, growth, temperature and the natural mortality of marine fish. *Fish Fish* **11**, 149–158 (2010).
72. Rogers, A., Blanchard, J. L. & Mumby, P. J. Fisheries productivity under progressive coral reef degradation. *J. Appl. Ecol.* **55**, 1041–1049 (2018).
73. Chen, S. & Watanabe, S. Age dependence of natural mortality coefficient in fish population dynamics. *Nippon Suisan Gakkaishi* **55**, 205–208 (1989).
74. Lehodey, P., Senina, I. & Murtugudde, R. A spatial ecosystem and populations dynamics model (SEAPODYM)—modeling of tuna and tuna-like populations. *Prog. Oceanogr.* **78**, 304–318 (2008).
75. Halfter, S., Cavan, E. L., Butterworth, P., Swadling, K. M. & Boyd, P. W. Sinking dead—how zooplankton carcasses contribute to particulate organic carbon flux in the subantarctic Southern Ocean. *Limnol. Oceanogr.* **67**, 13–25 (2021).
76. Saba, G. K. & Steinberg, D. K. Abundance, composition and sinking rates of fish fecal pellets in the Santa Barbara Channel. *Sci. Rep.* **2**, 716 (2012).
77. Siegel, D. A., DeVries, T., Doney, S. C. & Bell, T. Assessing the sequestration time scales of some ocean-based carbon dioxide reduction strategies. *Environ. Res. Lett.* **16**, 104003 (2021).
78. Primeau, F. Characterizing transport between the surface mixed layer and the ocean interior with a forward and adjoint global ocean transport model. *J. Phys. Oceanogr. J. Phys. Oceanogr.* <https://doi.org/10.1175/JPO2699.1> (2005).

79. R. Core Team. *R: A Language and Environment for Statistical Computing* (R Foundation for Statistical Computing, Vienna); <https://www.R-project.org/> (2021).
80. Mariani, G. et al. The combined impact of fisheries and climate change on future carbon sequestration by oceanic macrofauna, GaelMariani/Projection-paper: Future carbon sequestration by oceanic macrofauna. zenodo <https://doi.org/10.5281/zenodo.17085415> (2025).

Acknowledgements

Funding was provided through the PhD scholarship from the University of Montpellier to G.M. and the Scholarship of La Fondation de la Mer (France) to G.M. Work by G.M. was also partially funded by the European Union under grant agreement no. 101083922 (OceanICU). Views and opinions expressed are however those of the author(s) only and do not necessarily reflect those of the European Union or European Research Executive Agency. Neither the European Union nor the granting authority can be held responsible for them. JG and DB acknowledge support from the National Aeronautics and Space Administration grant 80NSSC25K7430, and computational resources from the Expanse system at the San Diego Supercomputer Center through allocation TG-OCE170017 from the Advanced Cyber infrastructure Coordination Ecosystem: Services and Support (ACCESS) program, which is supported by National Science Foundation grants 2138259, 2138286, 2138307, 2137603, and 2138296.

Author contributions

Conceptualization: G.M., M.T. and D.M. Methodology: G.M., J.G., D.B., T.D., M.T. and D.M. Software: G.M., J.G., D.B., T.D. and N.B. Formal analysis and investigation: G.M. Resources: G.M., J.G., D.B. and T.D. Writing—original draft: G.M., M.T. and D.M. Writing—review and editing: G.M., J.G., D.B., T.D., M.T. and D.M. Visualization: G.M.

Competing interests

The authors declare no competing interests.

Additional information

Supplementary information The online version contains supplementary material available at <https://doi.org/10.1038/s41467-025-64576-8>.

Correspondence and requests for materials should be addressed to Gaël. Mariani.

Peer review information *Nature Communications* thanks Daniel Ottmann and Oswald Schmitz for their contribution to the peer review of this work. A peer review file is available.

Reprints and permissions information is available at <http://www.nature.com/reprints>

Publisher's note Springer Nature remains neutral with regard to jurisdictional claims in published maps and institutional affiliations.

Open Access This article is licensed under a Creative Commons Attribution-NonCommercial-NoDerivatives 4.0 International License, which permits any non-commercial use, sharing, distribution and reproduction in any medium or format, as long as you give appropriate credit to the original author(s) and the source, provide a link to the Creative Commons licence, and indicate if you modified the licensed material. You do not have permission under this licence to share adapted material derived from this article or parts of it. The images or other third party material in this article are included in the article's Creative Commons licence, unless indicated otherwise in a credit line to the material. If material is not included in the article's Creative Commons licence and your intended use is not permitted by statutory regulation or exceeds the permitted use, you will need to obtain permission directly from the copyright holder. To view a copy of this licence, visit <http://creativecommons.org/licenses/by-nc-nd/4.0/>.

© The Author(s) 2025